INTERNATIONAL JOURNAL OF OPTIMIZATION IN CIVIL ENGINEERING
Int. J. Optim. Civil Eng., 2025; 15(2):259-278

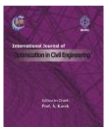

TUNED METAHEURISTIC ALGORITHMS FOR OPTIMAL DESIGN PROBLEMS WITH CONTINUOUS VARIABLES

A. Kaveh[*, †] and A. Eskandari
School of Civil Engineering, Iran University of Science and Technology, Narmak, Tehran, Iran

[DOI: 10.22068/ijoce.2025.15.2.637]

ABSTRACT

Metaheuristic algorithms mostly consist of some parameters influencing their performance when faced with various optimization problems. Therefore, this paper applies Multi-Stage Parameter Adjustment (MSPA), which employs Extreme Latin Hypercube Sampling (XLHS), Primary Optimizer, and Artificial Neural Networks (ANNs) to a recently developed algorithm called the African Vulture Optimization Algorithm (AVOA) and a well-known one named Particle Swarm Optimization (PSO) for tuning their parameters. The performance of PSO is tested against two engineering and AVOA for two structural optimization problems, and their corresponding results are compared to those of their default versions. The results showed that the employment of MSPA improved the performance of both metaheuristic algorithms in all the considered optimization problems.

Keywords: Metaheuristics, Optimization, Multi-Stage Parameter Adjustment, Artificial Neural Networks, Extreme Latin Hypercube Sampling, AVOA, PSO.

Received: 24 April 2025; Accepted: 28 June 2025

1. INTRODUCTION

Optimization plays a pivotal role in civil engineering and has been widely applied across various disciplines, including engineering design, computer science, and economics, where it is utilized to address complex problems that lack efficient solutions [1]. Numerous optimization algorithms have been proposed to enhance problem-solving efficiency in computational contexts, particularly when tackling challenging structural and engineering design problems [2]. Metaheuristic algorithms, in particular, have emerged as effective tools

[*]Corresponding author: School of Civil Engineering, Iran University of Science and Technology, Narmak, Tehran, Iran
[†]E-mail address: alikaveh@iust.ac.ir (A. Kaveh)

for solving these problems due to their ability to explore vast solution spaces in search of near-optimal solutions. However, the success of metaheuristics in structural optimization tasks is contingent upon the careful tuning of their initial parameters, a process that often demands significant time and effort [3]. The initialization of these parameters directly influences the algorithm's performance, determining the balance between exploration and exploitation of the search space, which is crucial for achieving optimal results [4].

Over the years, substantial research has been dedicated to understanding and refining the parameterization of various metaheuristic algorithms, such as Particle Swarm Optimization (PSO) [5,6], Ant Colony Optimization (ACO) [7,8], and Artificial Bee Colony (ABC) [9,10], among others. Each of these algorithms has specific parameters that require adjustment to enhance performance in specific applications. The significance of effective parameter tuning has led to the development of frameworks that optimize this process, such as the Multi-Stage Parameter Adjustment (MSPA) framework [11], which has been successfully employed to improve metaheuristics' efficiency in solving structural optimization problems. Despite this, achieving the ideal parameter configuration remains a labor-intensive and complex task, as the search for optimal values can vary greatly depending on the nature of the problem being addressed.

In this context, this paper applies the MSPA framework for parameter tuning of two metaheuristic algorithms, namely Particle Swarm Optimization and African Vultures Optimization Algorithm [12]. The proposed framework, which involves four stages: data generation, parameter optimization, machine learning-based training, and final optimization, leverages the advantages of Extreme Latin Hypercube Sampling (XLHS) for efficient exploration of search spaces and the predictive power of machine learning algorithms for parameter fine-tuning. By integrating machine learning with metaheuristics, this method offers the potential for substantial improvements in the design and optimization of engineering structures. This paper aims to explore the application of this framework to various engineering and structural optimization problems, demonstrating its efficacy in achieving enhanced performance and more efficient parameter tuning.

The structure of this paper is as follows: Section 2 provides a brief overview of Multi-Stage Parameter Adjustment. Section 3 delves into the description of the considered algorithms for parameter adjustment and optimization. Section 4 presents a series of case studies to highlight the effectiveness of the proposed approach, while Section 5 concludes the study with a summary of key findings.

2. MULTI-STAGE PARAMETER ADJUSTMENT (MSPA)

This study employs the recently developed Metaheuristic Parameter Adjustment (MSPA) framework, which enhances metaheuristic optimization performance through systematic parameter tuning [11]. The MSPA framework integrates three key components: Extreme Latin Hypercube Sampling (XLHS), a Primary Optimizer, and Machine Learning techniques for metaheuristic parameter optimization. The initial phase involves data generation using XLHS, a novel sampling method introduced by Kaveh and Eskandari [11].

Extreme Latin Hypercube Sampling (XLHS) derives its name from its conceptual foundation in Latin Hypercube Sampling (LHS) [13], yet it introduces an advanced

[DOI: 10.22068/ijoce.2025.15.2.637]

partitioning strategy to improve search space coverage. Unlike conventional approaches such as Full Factorial Design (FFD) and its variants, which are predominantly suited for discrete variables [14], XLHS ensures comprehensive exploration of the parameter space while simultaneously producing a robust dataset suitable for machine learning applications. The methodology involves segmenting the parameter space into distinct subspaces, followed by the strategic placement of sample points to achieve optimal coverage across all possible combinations. This feature is particularly beneficial in scenarios requiring high-quality training data for predictive modeling. Figure 1 demonstrates the XLHS approach in a two-dimensional space, where the domain is partitioned, and 20 sample points are randomly generated within each subspace to form the initial population for subsequent optimization runs.

Following the sampling phase, MSPA utilizes a Primary Optimizer, a metaheuristic algorithm with fixed parameters, such as Genetic Algorithm (GA) [15] or Colliding Bodies Optimization (CBO) [16], to optimize the parameters of the secondary (main) metaheuristic. In this work, two primary optimizers are employed: a hybrid CBO-GA algorithm, as proposed in [17], and a standard GA. The procedural steps of these optimizers are detailed in Figures 2 and 3.

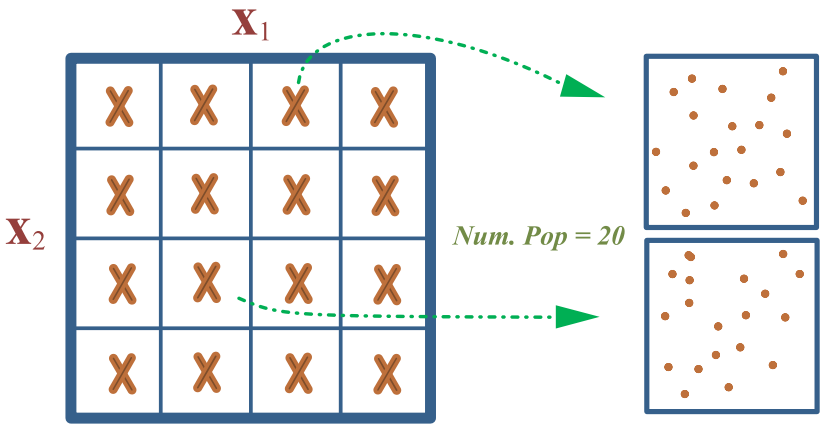

Figure 1: Extreme Latin Hypercube Sampling

Artificial Neural Networks (ANNs) [18,19], illustrated in Figure 4, are robust computational tools extensively applied in civil engineering, particularly in structural optimization [20]. Additionally, ANNs have been widely utilized for predictive modeling in structural engineering [21]. In this study, ANNs are developed to forecast optimal parameters, followed by structural optimization. For a comprehensive exposition, the step-by-step process is delineated in Figure 5.

3. METAHEURISTIC ALGORITHMS

This research focuses on tuning two metaheuristic algorithms, Particle Swarm Optimization (PSO), selected for its broad applicability, and the African Vulture Optimization Algorithm (AVOA), using the MSPA framework for optimal design problems. Subsequently, the tuned

[DOI: 10.22068/ijoce.2025.15.2.637]

variants are benchmarked against their original counterparts. A concise overview of these algorithms is provided below.

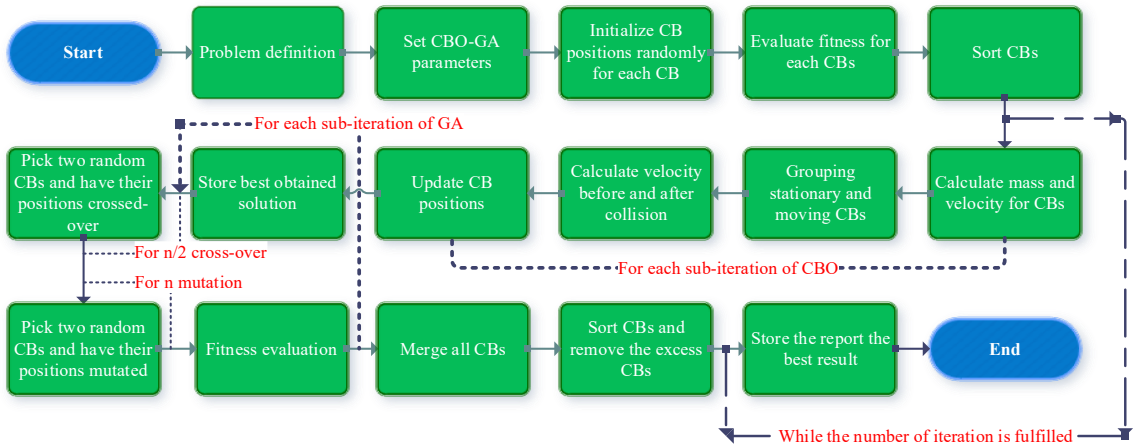

Figure 2: Flowchart of CBO-GA

Figure 3: Flowchart of GA

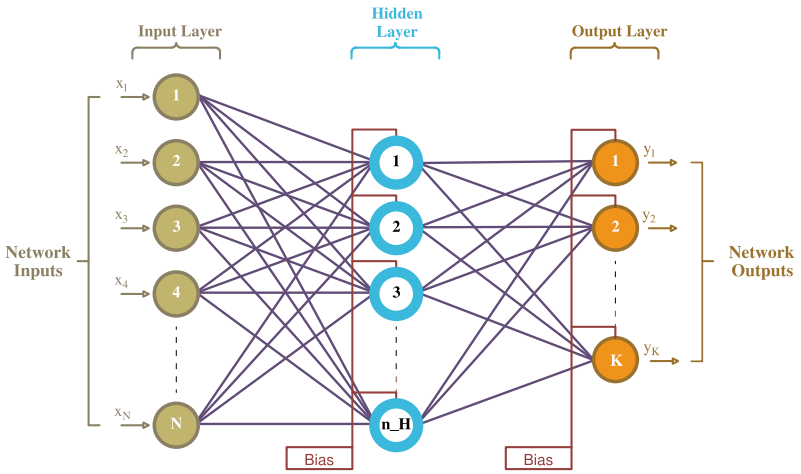

Figure 4: Structure of an ANN

3.1. African Vulture Optimization Algorithm (AVOA)

Introduced by Abdollahzadeh et al. [12] in 2021, AVOA is a bio-inspired metaheuristic algorithm that emulates the foraging and competitive behaviors of African vultures. The algorithm effectively balances exploration and exploitation by simulating vultures' interactions around food sources (carrion). Operating within a population-based framework, AVOA employs competitive mechanisms among agents to converge toward optimal

[DOI: 10.22068/ijoce.2025.15.2.637]

solutions [22]. Figure 6 outlines the core principles of AVOA, aligning them with vulture behavior, while Table 1 presents the corresponding mathematical formulations.

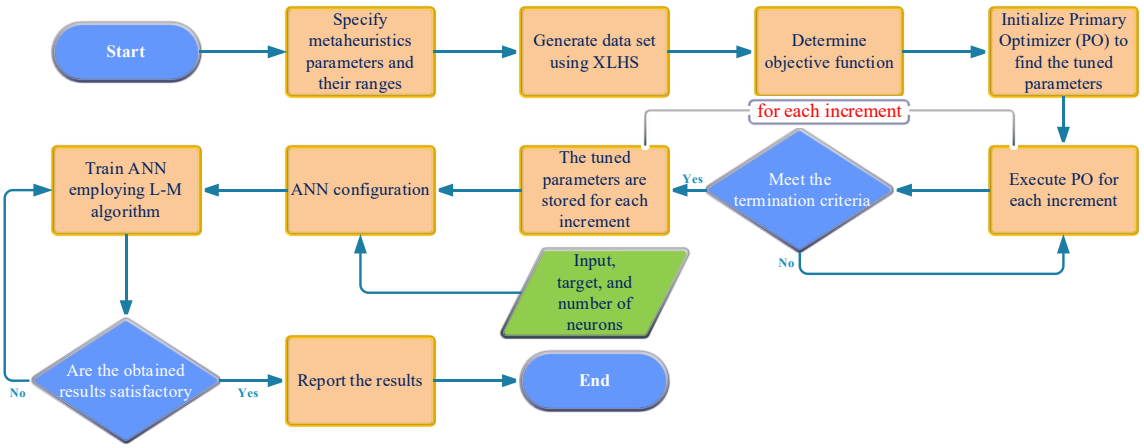

Figure 5: Workflow of MSPA

3.2. Particle Swarm Optimization (PSO)

Developed by Eberhart and Kennedy [5], Particle Swarm Optimization (PSO) is a stochastic, population-based optimization technique inspired by the collective motion of bird flocks or fish schools. The algorithm initializes a swarm of particles distributed randomly across the search space. Each particle navigates the search domain via velocity vectors, dynamically adjusted based on three factors:

1. The particle's personal best position ($pbest$)
2. The global best position ($gbest$) attained by the swarm
3. The particle's current velocity

The position update for particle i at iteration $(t+1)$ follows these equations:

$$x^i(t+1) = x^i(t) + dv^i(t+1) \tag{1}$$

$$dv^i(t+1) = \omega dv^i(t) + c_1 r_1 \left(pbest^i(t) x^i(t)\right) + c_2 r_2 \left(gbest(t) x^i(t)\right) \tag{2}$$

where:

- $x_i(t)$ and $v_i(t)$ denote the position and velocity of particle i at iteration t.
- $pbest^i$ and $gbest$ represent the particle's local best and the swarm's global best positions, respectively.
- r_1,r_2 are uniformly distributed random numbers in [0,1][0,1].
- c_1,c_2 are acceleration coefficients.
- ω is the inertia weight governing momentum retention.

[DOI: 10.22068/ijoce.2025.15.2.637]

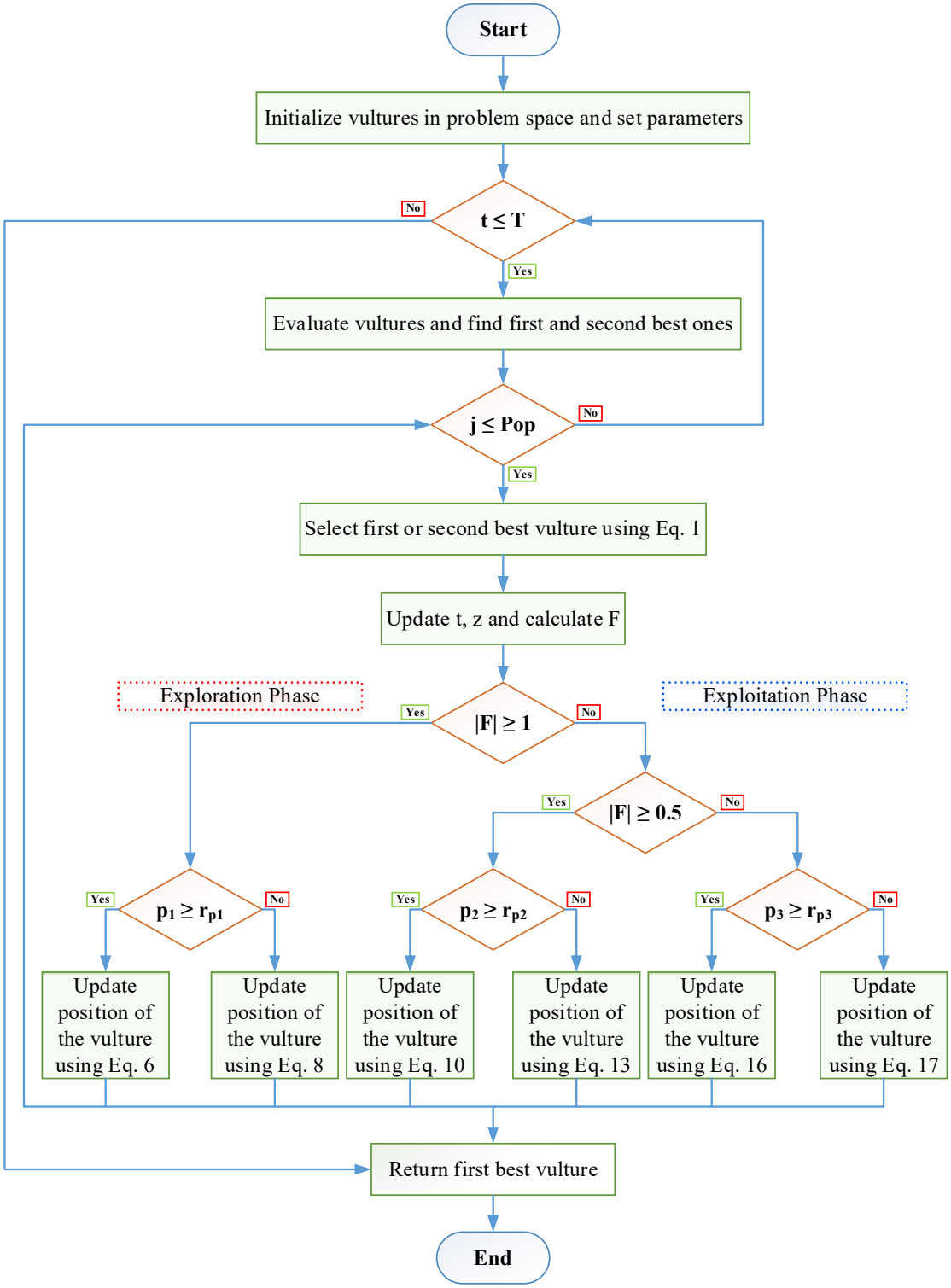

Figure 6: Flowchart of African Vulture Optimization Algorithm

[DOI: 10.22068/ijoce.2025.15.2.637]

Table 1: AVOA equations

Num.	Equation	Description
1	$R(i)=\begin{cases}Best\ vulture\ 1 & if \quad p_i=L_1\\ Best\ vulture\ 2 & if \quad p_i=L_2\end{cases}$	Determining the best vulture in any group
2	$P_i=\frac{F_i}{\sum_{i=1}^{n}F_i}$	Roulette wheel selection
3	$t=h\times\left(\sin^{w}\left(\frac{\pi}{2}\times\frac{Iteration\ i}{max\ Iteration}\right)+cos\left(\frac{\pi}{2}\times\frac{Iteration\ i}{max\ Iteration}\right)-1\right)$	Vultures' rate of starvation
4	$F=(2\times rand_1+1)\times z\times\left(1-\frac{Iteration_i}{max\ Iteration}\right)+t$	Vultures' satiety status
5	$P(i+1)=\begin{cases}Equation\ (6) & if \quad P_1\geq rand_{p_1}\\ Equation\ (8) & if \quad P_1<rand_{p_1}\end{cases}$	Exploration
6 7	$P(i+1)=R(i)-D(i)\times F$ $D(i)=\lvert X\times R(i)-P(i)\rvert$	Exploration #1
8	$P(i+1)=R(i)-F+rand_2\times\left((ub-lb)\times rand_3+lb\right)$	Exploration #2
9	$P(i+1)=\begin{cases}Equation\ (10) & if \quad P_2\geq rand_{p_2}\\ Equation\ (13) & if \quad P_2<rand_{p_2}\end{cases}$	Exploitation
10 11	$P(i+1)=D(i)\times(F+rand_4)-d(t)$ $d(t)=R(i)-P(i)$	Food competition
12	$S_1=R(i)\times\left(\frac{rand_5\times P(i)}{2\pi}\right)\times\cos\left(P(i)\right)$ $S_2=R(i)\times\left(\frac{rand_6\times P(i)}{2\pi}\right)\times\sin\left(P(i)\right)$	Rotating flight of vultures
13	$P(i+1)=R(i)-(S_1+S_2)$	
14	$P(i+1)=\begin{cases}Equation\ (16) & if \quad P_3\geq rand_{p_3}\\ Equation\ (17) & if \quad P_3<rand_{p_3}\end{cases}$	Exploitation (second phase)
15	$A_1=BestVulture_1(i)-\frac{BestVulture_1(i)\times P(i)}{BestVulture_1(i)-P(i)^2}\times F$ $A_2=BestVulture_2(i)-\frac{BestVulture_2(i)\times P(i)}{BestVulture_2(i)-P(i)^2}\times F$	Accumulation of several types of vultures over the food source
16	$P(i+1)=\frac{A_1+A_2}{2}$	
17	$P(i+1)=R(i)-\lvert d(t)\rvert\times F\times Levy(d)$	Aggressive Competition for Food using Levy flight
18	$LF(d)=0{,}01\times\frac{u\times\sigma}{\lvert v\rvert^{\frac{1}{\beta}}}\quad .\quad \sigma=\left(\frac{\Gamma(1+\beta)\times\sin\left(\frac{\pi\beta}{2}\right)}{\Gamma(1+\beta2)\times\beta\times2\left(\frac{\beta-1}{2}\right)}\right)^{\frac{1}{\beta}}$	

[DOI: 10.22068/ijoce.2025.15.2.637]

4. NUMERICAL EXAMPLES

In this section, various numerical examples, including engineering and structural optimization problems, are presented to evaluate the employment of the MSPA in improving the performance of the considered metaheuristic algorithms. The parameters of both algorithms, their ranges, and their suggested values, which were tuned employing the MSPA, are represented in Table 2. The constrained engineering design problems with continuous variables comprise tension/compression spring design and tree bar truss design. The structural constrained optimization examples with continuous variables are the 10-bar planar truss and the 25-bar transmission tower. To have a fair comparison, each of the default and tuned algorithms is executed 30 times independently, and their best cost, worst cost, mean, and standard deviation were obtained. Moreover, the best design related to the best cost of each is presented and compared to one another. The constraints are implemented employing the penalty function.

Table 2: Range and suggested values of the parameters

Algorithm	Parameter	Indicator	min	max	Suggested	
AVOA	L_1	First Best Vulture Selection	0	1	0.8	[22]
	L_2	Second Best Vulture Selection	0	1	0.2	
	w	Exploration or Exploitation Selection	2	3	2.5	
	P_1	Exploration Phase	0	1	0.6	
	P_2	First Exploitation Phase	0	1	0.4	
	P_3	Second Exploitation Phase	0	1	0.6	
PSO	A_1	Inertia weight (velocity impact)	0.8	1.2	1	
	A_2	Damping ratio	0	1	0.99	
	A_3	c_1 (cognitive parameter)	1	3	2	
	A_4	c_2 (social parameter)	1	3	2	

The regression plots for the ANN-PSO (Figure 7) and ANN-AVOA (Figure 8) models demonstrate robust predictive accuracy, as evidenced by their near-perfect coefficients of determination ($R = 0.995$ and $R = 0.98855$, respectively). Both models exhibit tight clustering of data points along the ideal fit line ($Y = T$), with minimal deviation for the ±20% bounds ($Y = 0{,}8T$ and $Y = 1{,}2T$). This indicates high fidelity in parameter tuning, where the ANN successfully captures the nonlinear relationships between input variables and optimized outputs. The consistency across training, validation, and test subsets confirms negligible overfitting, suggesting generalizability to unseen data. For ANN-PSO, the marginally higher R-value highlights slightly superior convergence stability compared to ANN-AVOA, though both achieve engineering-grade precision.

The output distributions (Figure 8) reveal that ANN-AVOA maintains strong agreement with target values across a range (0.5–2.5), with no systematic bias. However, minor scatter at higher targets ($Y \geq 2$) suggests localized sensitivity to parameter thresholds, possibly due to AVOA's adaptive exploration-exploitation balance. In contrast, ANN-PSO's tighter error bounds (Figure 7) imply more uniform performance, aligning with PSO's gradient-aware particle dynamics. Both models' adherence to the ±20% tolerance bands underscores their reliability for metaheuristic hyperparameter optimization, with ANN-PSO offering marginally better precision for high-stakes applications requiring stringent error control.

[DOI: 10.22068/ijoce.2025.15.2.637]

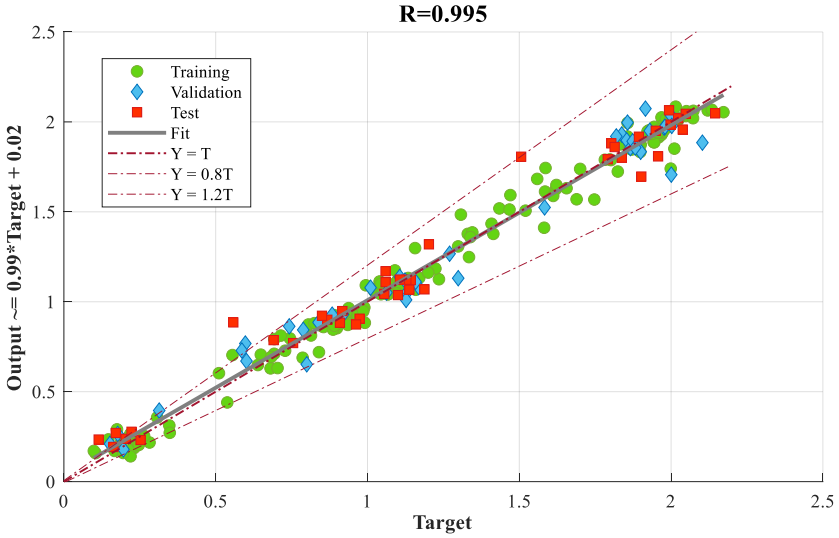

Figure 7: Regression for Training, Validation, and Test of the ANN–PSO

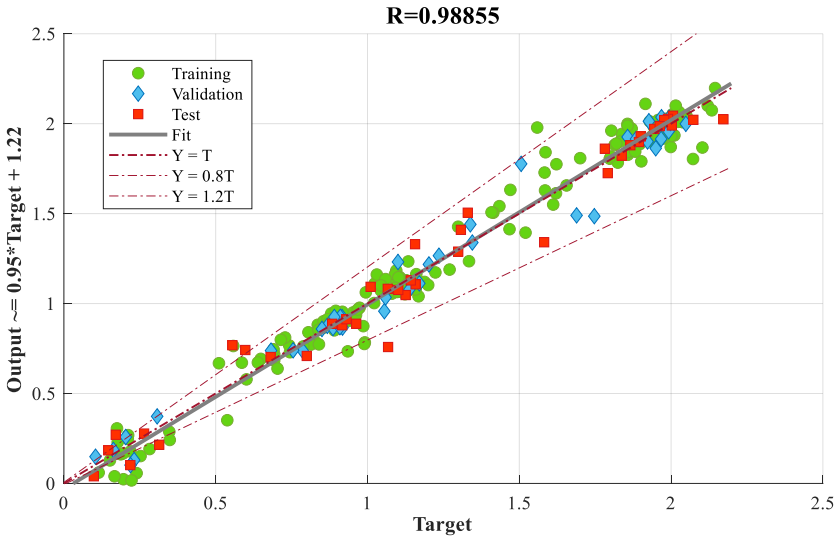

Figure 8: Regression for Training, Validation, and Test of the ANN–AVOA

4.1. Tension/compression spring design

The initial problem at hand revolves around the endeavor to minimize the weight of the spring, as visually depicted in Figure 9, while subjected to specified constraints. These constraints encompass outside diameter thresholds, frequency limitations, minimum deflection requirements, and shear stress. This design problem was initially described by Belegundu et al. [23]. The problem has three distinct design variables, namely d or x_1 (representing wire diameter), D or x_2 (denoting coil diameter), and N or x_3 (indicating the number of active coils). The ensuing mathematical model represents the

[DOI: 10.22068/ijoce.2025.15.2.637]

tension/compression spring design problem.

Consider $\vec{X} = [x_1.x_2.x_3] = [D.d.N]$

Minimize $f_{cost}(\vec{X}) = (x_3 + 2)x_2x_1^2$

Subjected to:

$$g_1(\vec{X}) = 1 - \frac{x_2^3 x_3}{71785x_1^4} \leq 0$$
$$g_2(\vec{X}) = \frac{4x_2^2 - x_1x_2}{12566(x_2x_1^3 - x_1^4)} + \frac{1}{5108x_1^2} \leq 0$$
$$g_3(\vec{X}) = 1 - \frac{140{,}45x_1}{x_2^2x_3} \leq 0 \qquad (3)$$
$$g_4(\vec{X}) = \frac{x_1 + x_2}{1{,}5} - 1 \leq 0$$
$$0{,}05 \leq x_1 \leq 2. \qquad 0{,}25 \leq x_2 \leq 1{,}3. \qquad 2 \leq x_3 \leq 15$$

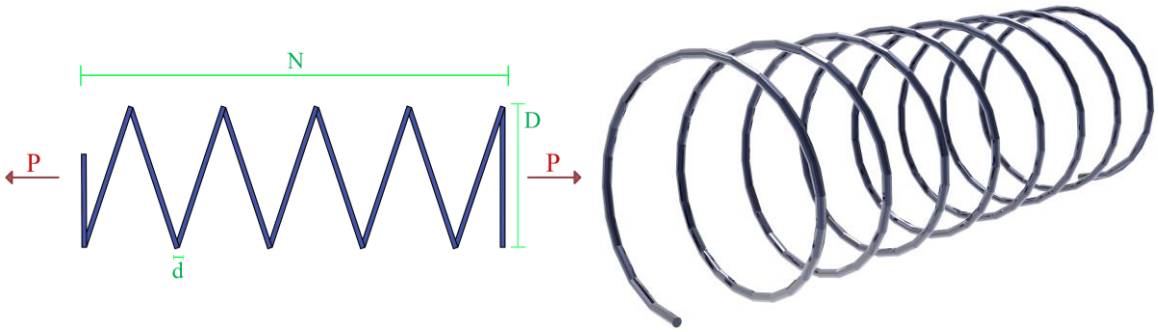

Figure 9: Tension/Compression Spring

As can be observed in Table 3, which provides the statistical results of default and adjusted PSO for the tension/compression spring, after parameter adjustment, PSO could show better performance in all aspects, such as best and worst cost, average, and standard deviation (almost 4%, 19%, 8.5%, and 65% improvement, respectively. Besides, its convergence rate was enhanced so that it could reach a better cost sooner, as shown in Figure 10.

Table 3: Comparison of Statistical Results and Best Designs for Spring Design

	Cost				**Best Design**		
	Best	Worst	Mean	Std.	x_1	x_2	x_3
Default	0.01318178	0.017638125	0.014259806	0.001161063	0.057186966	0.503976707	5.997780213
Tuned	**0.012665233**	**0.014344222**	**0.013050625**	**0.000408962**	**0.051694801**	**0.356855839**	**11.28087402**

[DOI: 10.22068/ijoce.2025.15.2.637]

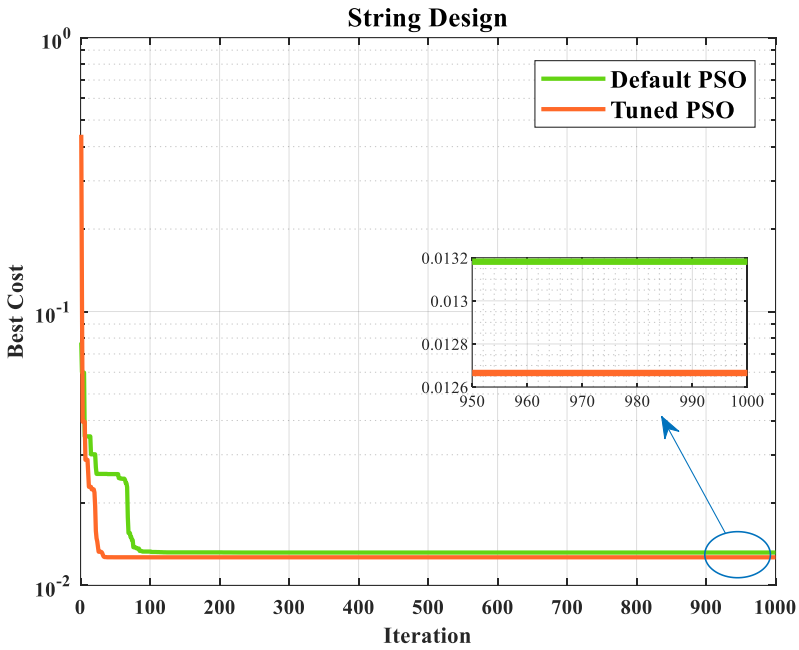

Figure 10: Performance Comparison for Spring Design

4.2. Three-bar truss design

This benchmark within the realm of structural engineering was initially posited by [24]. As depicted in Figure 11, the truss structure exhibits a triad of bar elements arranged symmetrically. The design variables under scrutiny pertain to the cross-sectional areas of these elements A_1 and A_2 as x_1 and x_2. The primary aim of this endeavor is to ascertain the structure's minimal weight, all while adhering to the stress constraints. The mathematical model of this optimization problem is thus articulated as follows.

Consider $\vec{X} = [x_1.x_2] = [A_1.A_2]$

Minimize $f_{cost}(\vec{X}) = (2\sqrt{2}x_1 + x_2) \times l$

Subjected to:

$$g_1(\vec{X}) = \frac{\sqrt{2}x_1 + x_2}{\sqrt{2}x_1^2 + 2x_1x_2} P - \sigma \leq 0$$
$$g_2(\vec{X}) = \frac{1}{x_1 + \sqrt{2}x_2} P - \sigma \leq 0 \quad (4)$$
$$g_3(\vec{X}) = \frac{x_2}{\sqrt{2}x_1^2 + 2x_1x_2} P - \sigma \leq 0$$

$$D = 100\ cm. P = 2kN/cm^2. \sigma = 2kN/cm^2 \quad \text{and} \quad 0 \leq x_1.x_2 \leq 1$$

[DOI: 10.22068/ijoce.2025.15.2.637]

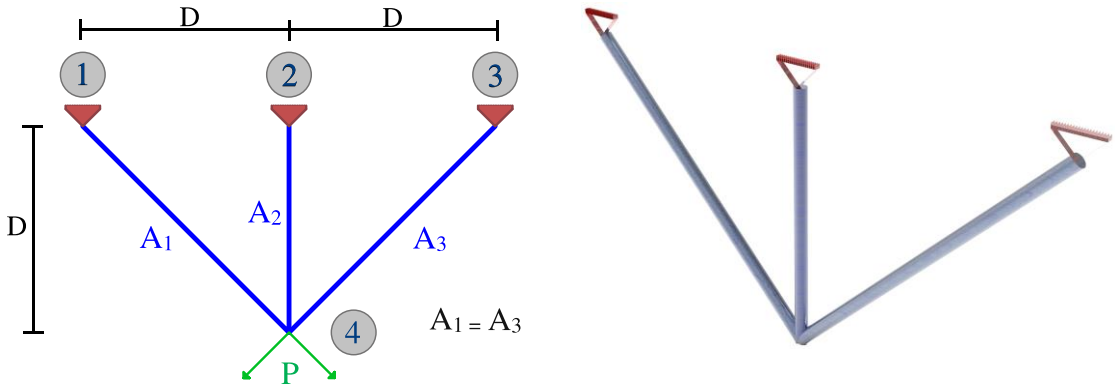

Figure 11: Three-Bar Truss

Based on the obtained results of the tree bar truss in Table 4, the application of parameter adjustment resulted in a better performance; however, this improvement is not that significant in the best cost, but it is remarkable in the standard deviation, which was enhanced by up to 83.3 %. Furthermore, the convergence of the adjusted PSO was better after almost 50 iterations, as depicted in Figure 12.

Table 4: Comparison of Statistical Results and Best Designs for Three-Bar Truss Design

	Cost				Best Design	
	Best	Worst	Mean	Std.	x_1	x_2
Default	263.89584500	263.89943151	263.89617708	0.00074472	0.78862814	0.40838122
Adjusted	**263.89584338**	**263.89622776**	**263.89595676**	**0.00012401**	**0.78867291**	**0.40825459**

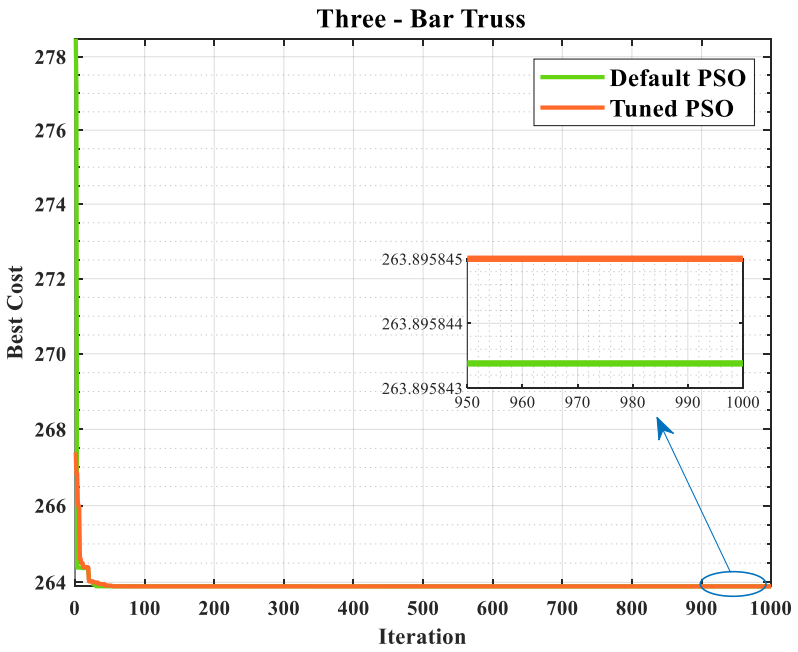

Figure 12: Performance Comparison for Three-Bar Truss Design

[DOI: 10.22068/ijoce.2025.15.2.637]

4.3. The 10-bar planar truss

The first structural optimization problem under investigation pertains to a planar truss. The arrangement of the 10-bar truss structure is illustrated in Figure 13, while Table 5 provides an overview of the design parameters. A singular loading condition, characterized by P = 100 kips, is imposed upon the structure.

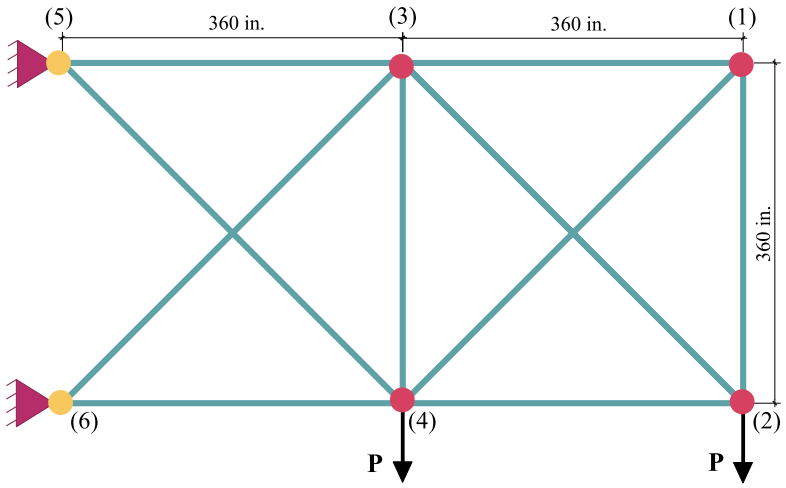

Figure 13: The 10-bar Planar Truss

Table 5: Design parameters of the 10-bar planar truss

Property	Value
Number of design variables	10
Mass density	0.1 lb/in^3
Elastic modulus	10,000 ksi
Allowable range for the cross-sectional area	0.1–35 in^2
Allowable stresses for all members	±25 ksi
Allowable nodal displacements	±2 in

The comparative analysis of the 10-bar planar truss optimization using both the default AVOA and the AAVOA (tuned via MSPA) reveals significant improvements in structural efficiency and algorithmic reliability. As illustrated in Table 6, AAVOA achieved a superior best weight of 5060.958 lb compared to AVOA's 5070.249 lb, alongside a lower mean weight (5206.486 lb vs. 5430.624 lb) and reduced standard deviation (222.5627 vs. 386.6023), highlighting its enhanced consistency and convergence. Figure 15 further demonstrates that AAVOA maintains elemental stresses within allowable limits (tensile/compressive) more effectively, with stress ratios consistently below the 0.8 threshold, indicating optimal material utilization. The nodal displacement ratios in Figure 16 corroborate this, showing AAVOA's ability to minimize deformations while adhering to constraints.

The search history, as represented in Figure 14, underscores AAVOA's refined exploration-exploitation balance, with 30 independent runs converging to near-optimal solutions (best weights clustered at 0.5–3.0 lb intervals) and fewer outliers than AVOA, as also plotted in Figure 17. This stability is attributed to parameter tuning through the MSPA,

[DOI: 10.22068/ijoce.2025.15.2.637]

which mitigates premature convergence, a limitation observed in AVOA's wider weight distribution (e.g., worst weight of 6204.354 lb vs. AAVOA's 5981.962 lb). The stress distribution patterns (Figure 15) and statistical results collectively validate AAVOA's superior robustness for truss optimization, particularly in scenarios demanding strict compliance with stress and displacement constraints. These findings position AAVOA as a preferred choice for complex structural optimization tasks requiring high precision and computational efficiency.

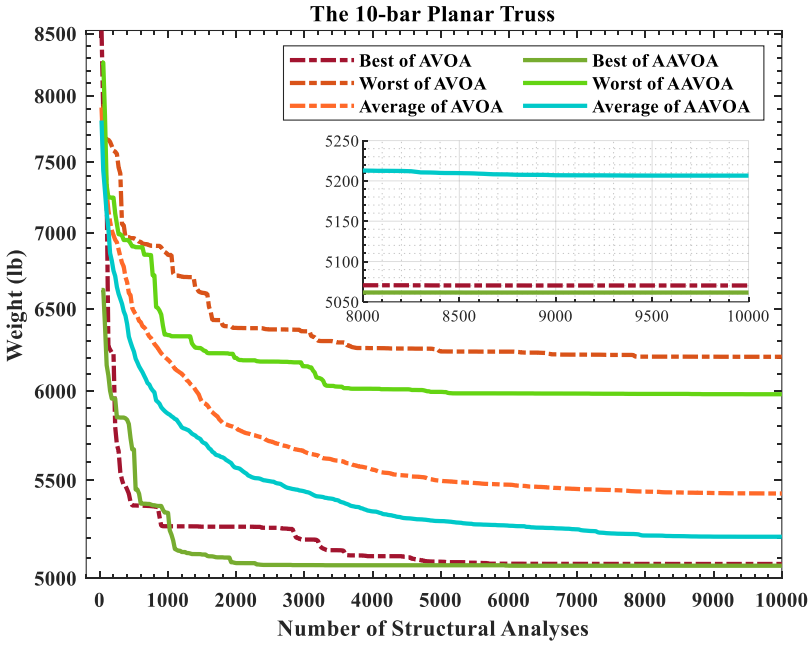

Figure 14: Performance Comparison for the 120-bar Dome Truss

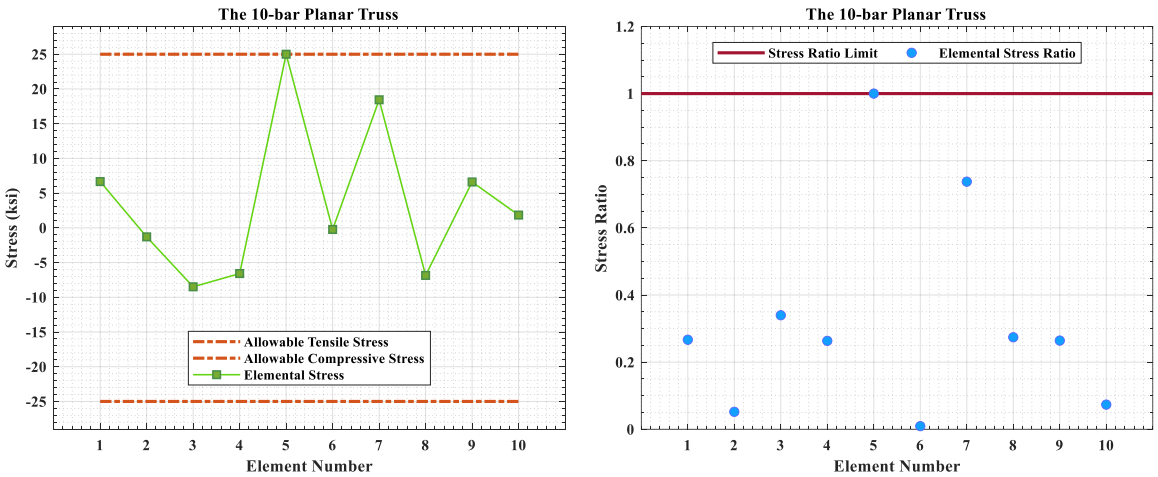

Figure 15: The 10-bar Planar Truss Elemental Stress and Stress Ratio

[DOI: 10.22068/ijoce.2025.15.2.637]

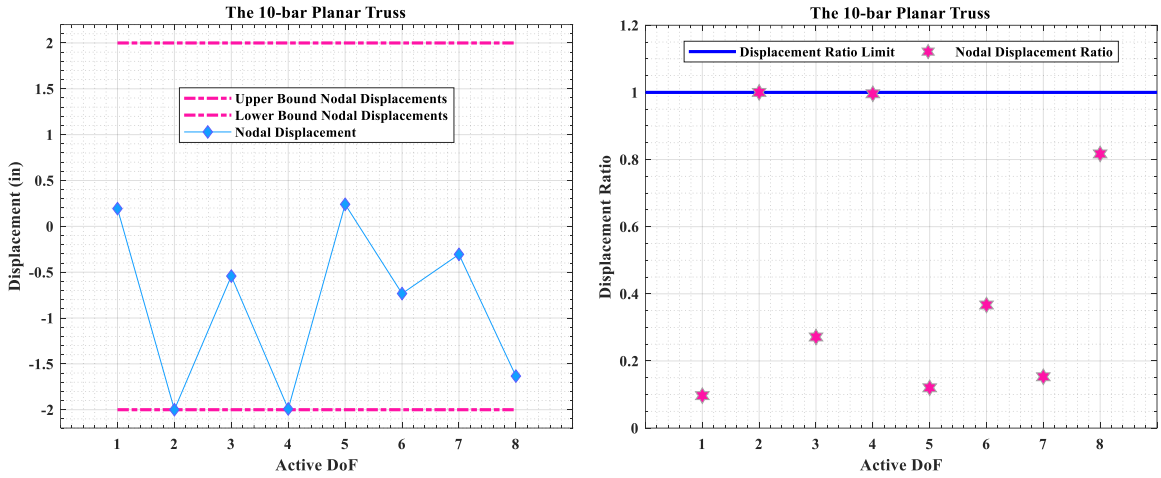

Figure 16: The 10-bar Planar Truss Nodal Displacement and Displacement Ratio

Table 6: Comparison of Statistical Results and Best Designs for the 10-bar Planar Truss

	Algorithm	
Element Group	AAVOA	AVOA
1	30.38928	30.26468
2	0.100002	0.1
3	23.24375	22.93433
4	15.20868	15.53487
5	0.1	0.133021
6	0.559178	0.437553
7	7.46777	7.426286
8	21.18442	21.48981
9	21.43914	21.49664
10	0.100001	0.1
Best Weight	**5060.958**	5070.249
Worst Weight	**5981.962**	6204.354
Mean	**5206.486**	5430.624
STD	**222.5627**	386.6023

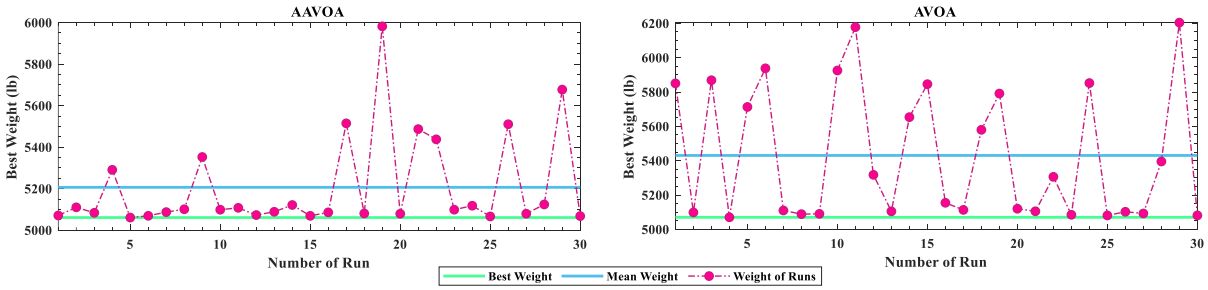

Figure 17: The 30 Independent Runs for the 10-bar Planar Truss

4.4. The 25-bar transmission tower

The other case study in this structural optimization analysis examines a 25-member spatial truss system, illustrated schematically in Figure 18. The material density, valued at

[DOI: 10.22068/ijoce.2025.15.2.637]

0.1 lb/in³ (equivalent to 2767.990 kg/m³), is accompanied by a modulus of elasticity set at 10,000 ksi (68,950 MPa). The arrangement of the twenty-five struts is subdivided into eight distinct groups. Within the framework of this benchmark tower truss, two specified load cases, detailed in Table 7, exert their respective influences. Stringent upper displacement bounds, fixed at 0.35 in (8.89 mm), are imposed uniformly across all nodal locations and dimensions. Axial stress constraints, outlined in Table 8, are variably specified across the categorized groups. The range of allowable cross-sectional areas spans from 0.01 in² to 3.4 in² (equivalent to 0.6452 cm² to 21.94 cm²).

Table 7: Loading Conditions for the 25-bar Tower.

	Case 1 (kips (kN))			Case 2 (kips (kN))		
Node	**P_X**	**P_Y**	**P_Z**	**P_X**	**P_Y**	**P_Z**
1	0.0	20.0 (89)	-5.0 (22.25)	1 (4.45)	10.0 (44.5)	-5.0 (22.25)
2	0.0	-20.0 (89)	-5.0 (22.25)	0	10.0 (44.5)	-5.0 (22.25)
3	0.0	0.0	0.0	0.5 (2.225)	0.0	0.0
6	0.0	0.0	0.0	0.5 (2.225)	0.0	0.0

Table 8: Member Stress Limitation for the 25-bar Transmission Tower

Element group	Compressive stress limitations (ksi (MPa))	Tensile stress limitations (ksi (MPa))
A1	35.092 (241.96)	40.0 (275.80)
A2 ~ A5	11.590 (79.913)	40.0 (275.80)
A6 ~ A9	17.305 (119.31)	40.0 (275.80)
A10 ~ A11	35.092 (241.96)	40.0 (275.80)
A12 ~ A13	35.092 (241.96)	40.0 (275.80)
A14 ~ A17	6.759 (46.603)	40.0 (275.80)
A18 ~ A21	6.959 (47.982)	40.0 (275.80)
A22 ~ A25	11.082 (76.410)	40.0 (275.80)

The comparative optimization results for the 25-bar transmission tower demonstrate the enhanced performance of the tuned AVOA (AAVOA) compared to the default AVOA. As evidenced in Table 9, AAVOA achieved a superior best weight of 545.18 lb versus AVOA's 546.23 lb, along with a lower average weight (549.17 lb vs. 554.34 lb) and significantly reduced standard deviation (2.91 lb vs. 7.39 lb), indicating more consistent convergence behavior. Figure 19 visually reinforces these findings, showing AAVOA's tighter clustering of optimal solutions across multiple runs. The elemental stress distribution in Figure 20 reveals that both algorithms maintained stresses within allowable limits, though AAVOA achieved this with 44.3% fewer structural analyses (4,800 vs. 8,625), highlighting its superior computational efficiency. This reduction in computational cost, coupled with improved weight optimization, makes AAVOA particularly valuable for large-scale structural design problems where both accuracy and efficiency are critical.

The 30 independent runs depicted in Figure 22 provide deeper insight into the algorithms' stability, with AAVOA exhibiting narrower weight distribution (557.12 lb worst case vs. AVOA's 576.72 lb) and reduced solution variability. This enhanced reliability stems from the MSPA parameter tuning, which effectively balances exploration and exploitation during the optimization process. The cross-sectional area allocations in Table 9 show that AAVOA produced more material-efficient designs, particularly in critical element groups, while

[DOI: 10.22068/ijoce.2025.15.2.637]

maintaining stress ratios well below unity (Figure 20). These results collectively demonstrate that AAVOA not only achieves lighter structures but does so with greater reproducibility and lower computational overhead, making it a robust choice for practical transmission tower optimization where both performance consistency and resource efficiency are paramount.

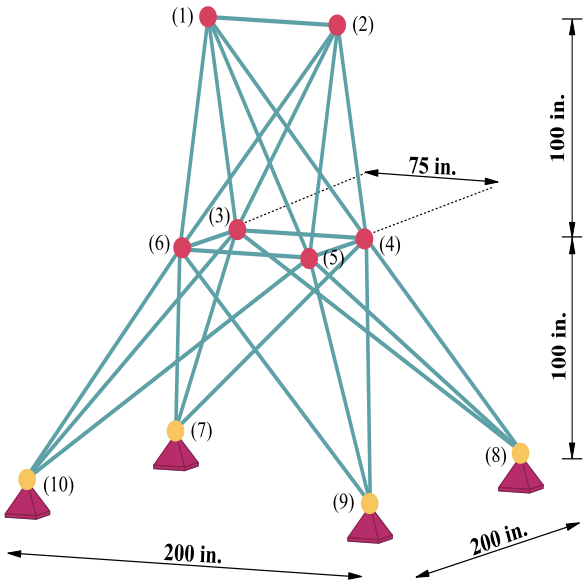

Figure 18: The 25-bar Transmission Tower

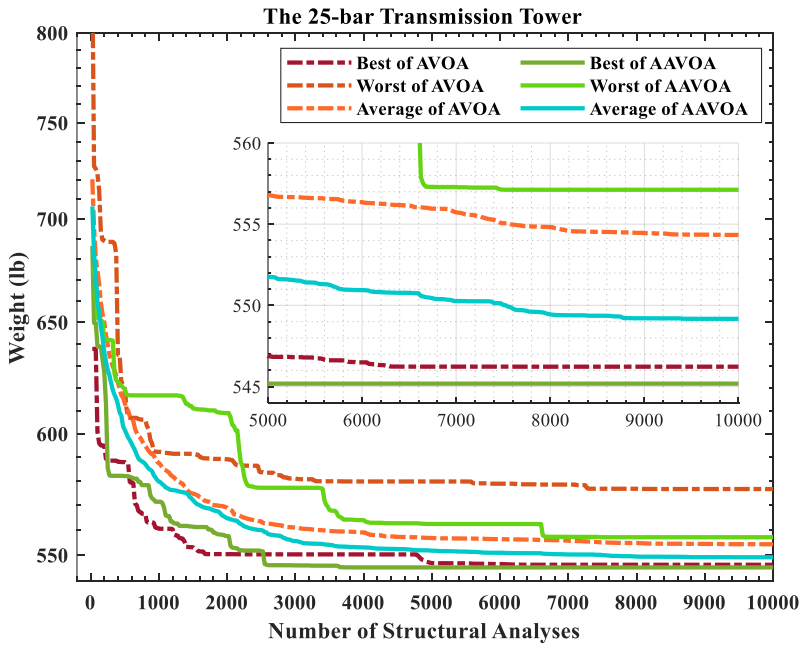

Figure 19: Performance Comparison for the 25-bar Transmission Tower

[DOI: 10.22068/ijoce.2025.15.2.637]

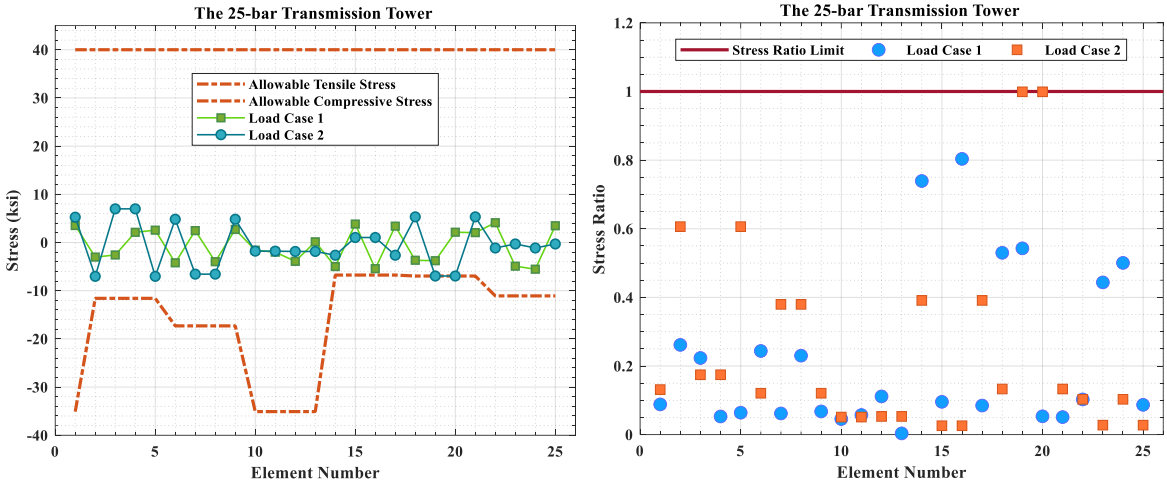

Figure 20: The 25-bar Transmission Tower Elemental Stress and Stress Ratio

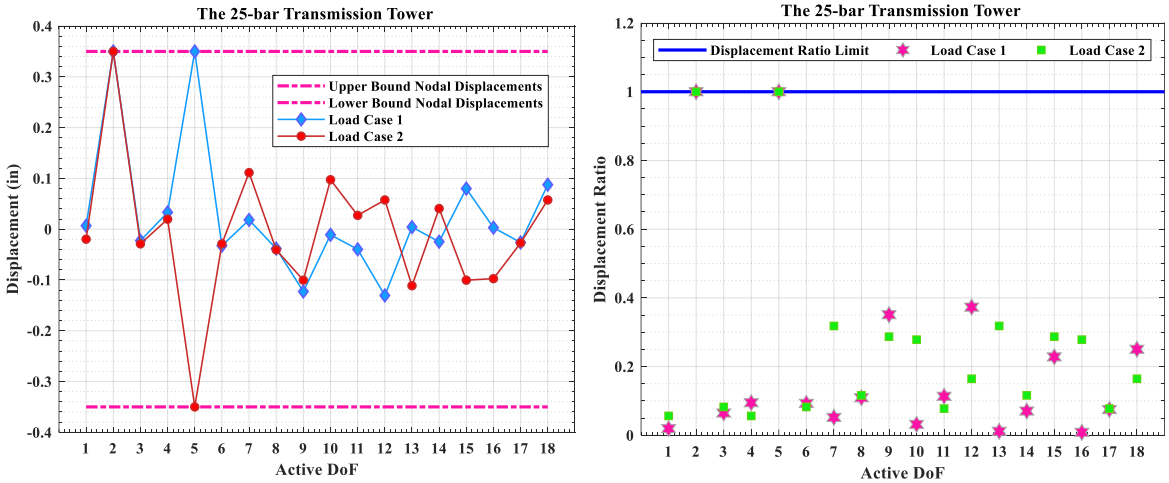

Figure 21: The 25-bar Transmission Tower Nodal Displacement and Displacement Ratio

Table 9: Comparison of Statistical Results and Best Designs for the 25-bar Transmission Tower

	Element groups	Algorithm	
		AVOA	**AAVOA**
1	A_1	0.01	0.01015267
2	A_2 -A_5	1.966856372	1.794516431
3	A_6 - A_9	3.021088499	3.262170844
4	A_{10} - A_{11}	0.010000358	0.010000002
5	A_{12} - A_{13}	0.010079984	0.01
6	A_{14} - A_{17}	0.684519132	0.686016472
7	A_{18} - A_{21}	1.681583427	1.736271621
8	A_{22} - A_{25}	2.653002619	2.57190571
Best Weight (lb)		546.2262918	**545.1820801**
Worst Weight (lb)		576.7215432	**557.1208098**
Average Weight (lb)		554.3397222	**549.1723122**
Standard Deviation (lb)		7.390827195	**2.914991611**
No. of Analyses		8625	**4800**

[DOI: 10.22068/ijoce.2025.15.2.637]

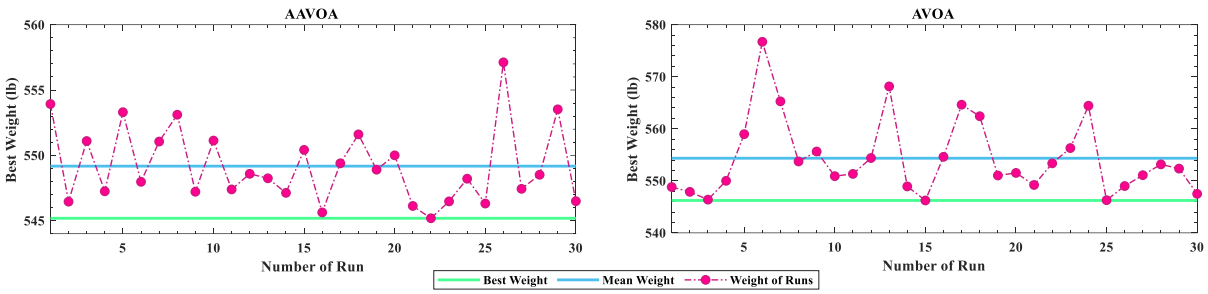

Figure 22: The 30 Independent Runs for the 25-bar Transmission Tower

5. CONCLUSIONS

This study employed a recently proposed framework, namely Multi-Stage Parameter Adjustment (MSPA), for enhancing two metaheuristic algorithms, including the African Vultures Optimization Algorithm (AVOA) and Particle Swarm Optimization (PSO), through systematic parameter tuning, demonstrating its efficacy in solving complex optimization problems with continuous variables. The proposed methodology integrates data generation, primary optimization, machine learning, and metaheuristic refinement to achieve superior performance across engineering and structural optimization benchmarks. By employing Extreme Latin Hypercube Sampling (XLHS) for exhaustive search space coverage and artificial neural networks (ANN) for predictive parameter tuning, MSPA significantly improved the convergence behavior and solution quality of metaheuristics such as PSO and AVOA. The results underscore the framework's versatility, with tuned algorithms outperforming their baseline counterparts in engineering problems and achieving lighter, more efficient designs in structural applications. Notably, the MSPA tuning reduced computational costs by up to 44.3% and 83.3% standard deviation while maintaining constraint satisfaction, highlighting MSPA's potential for real-world engineering design.

REFERENCES

1. Yang XS. *Engineering Optimization: An Introduction with Metaheuristic Applications*. John Wiley & Sons; 2010.

2. Kaveh A. *Advances in Metaheuristic Algorithms for Optimal Design of Structures*. Springer; 2014.
3. Eiben ÁE, Hinterding R, Michalewicz Z. Parameter control in evolutionary algorithms. *IEEE Trans Evol Comput*. 1999;**3**:124–41.
4. Bäck T, Schwefel HP. An overview of evolutionary algorithms for parameter optimization. *Evol Comput*. 1993;**1**:1–23.
5. Eberhart R, Kennedy J. Particle swarm optimization. In: *Proc IEEE Int Conf Neural Netw*. Citeseer; 1995:1942–48.
6. Iwasaki N, Yasuda K, Ueno G. Dynamic parameter tuning of particle swarm optimization. *IEEJ Trans Electr Electron Eng*. 2006;**1**:353–63.

[DOI: 10.22068/ijoce.2025.15.2.637]

7. Dorigo M, Birattari M, Stutzle T. Ant colony optimization. *IEEE Comput Intell Mag*. 2006;**1**:28–39.
8. Wong KY. Parameter tuning for ant colony optimization: A review. In: *2008 Int Conf Comput Commun Eng*. IEEE; 2008:542–45.
9. Karaboga D, Akay B. A comparative study of artificial bee colony algorithm. *Appl Math Comput*. 2009;**214**:108–32.
10. Akay B, Karaboga D. Parameter tuning for the artificial bee colony algorithm. In: *Comput Collect Intell*. Springer; 2009:608–19.
11. Kaveh A, Eskandari A. Multi-stage parameter adjustment to enhance metaheuristics for optimal design. *Acta Mech*. 2024;**235**:1–21.
12. Abdollahzadeh B, Gharehchopogh FS, Mirjalili S. African vultures optimization algorithm: A new nature-inspired metaheuristic algorithm for global optimization problems. *Comput Ind Eng*. 2021;**158**:107408.
13. McKay MD, Beckman RJ, Conover WJ. A comparison of three methods for selecting values of input variables in the analysis of output from a computer code. *Technometrics*. 2000;**42**:55–61.
14. Fisher RA. *The Design of Experiments*. Oliver & Boyd; 1966.
15. Sastry K, Goldberg D, Kendall G. Genetic algorithms. In: *Search Methodologies: Introductory Tutorials in Optimization and Decision Support Techniques*. 2005:97–125.
16. Kaveh A, Mahdavi VR. Colliding bodies optimization: A novel meta-heuristic method. *Comput Struct*. 2014;**139**:18–27.
17. Kaveh A, Eskandari A. Tuned African vultures optimization algorithm for optimal design of skeletal structures employing multi-stage parameter adjustment. *Iran J Sci Technol Trans Civ Eng*. 2025;**49**:1211–32.
18. Cherkassky V, Mulier FM. *Learning from Data: Concepts, Theory, and Methods*. John Wiley & Sons; 2007.
19. Jordan MI, Mitchell TM. Machine learning: Trends, perspectives, and prospects. *Science*. 2015;**349**:255–60.
20. Iranmanesh A, Kaveh A. Structural optimization by gradient-based neural networks. *Int J Numer Methods Eng*. 1999;**46**:297–311.
21. Shayanfar M, Zaherbin P, Niaraki PJ, Eskandari A. Force-displacement relation for lumped plasticity model of compact square concrete-filled steel tube columns. *Results Eng*. 2024;**23**:102619.
22. Sasmal B, Das A, Dhal KG, Saha R. A comprehensive survey on African vulture optimization algorithm. *Arch Comput Methods Eng*. 2023:1–42.
23. Belegundu AD, Arora JS. A study of mathematical programming methods for structural optimization. Part I: Theory. *Int J Numer Methods Eng*. 1985;**21**:1583–99.
24. Ray T, Saini P. Engineering design optimization using a swarm with intelligent information sharing among individuals. *Eng Optim*. 2001;**33**:735–48.

[DOI: 10.22068/ijoce.2025.15.2.637]